

---

# Evaluation of Geometric Sensitivity for Hybrid PET

Robert Z. Stodilka and Stephen J. Glick

*Department of Nuclear Medicine, University of Massachusetts Medical School, Worcester, Massachusetts*

---

Hybrid PET systems have spatially varying sensitivity profiles. These profiles are dependent on imaging parameters, namely, number of heads, head configuration, spacing between gantry stops, radius of rotation (RoR), and coincident head acceptance angle. **Methods:** Sensitivity profiles were calculated across a 500-mm field of view (FoV) for a representative set of existing and theoretic 2-, 3-, and 4-head hybrid PET systems. The head configuration was defined by  $\alpha_n$ , which describes the angular separation between head 1 and head  $n$ . Simulated configurations were 2 head ( $[\alpha_2] = [180^\circ]$ ), 3 head ( $[\alpha_2, \alpha_3] = [120^\circ, 240^\circ]$  and  $[90^\circ, 180^\circ]$ ), and 4 head ( $[\alpha_2, \alpha_3, \alpha_4] = [90^\circ, 180^\circ, 270^\circ]$ ). Four transverse acceptance angles, measured from the perpendicular of the crystal to the surface, were simulated:  $90^\circ$ ,  $45^\circ$ ,  $23^\circ$ , and  $11^\circ$ . Two RoRs were considered: 250 and 300 mm. Each head was rotated through  $360^\circ$  in 128 steps, and no physical collimation was modeled. **Results:** For a 250-mm RoR and  $90^\circ$  acceptance angle, the sensitivities relative to  $[\alpha_2] = [180^\circ]$  were  $[\alpha_2, \alpha_3] = [120^\circ, 240^\circ]$ , 183%;  $[\alpha_2, \alpha_3] = [90^\circ, 180^\circ]$ , 159%; and  $[\alpha_2, \alpha_3, \alpha_4] = [90^\circ, 180^\circ, 270^\circ]$ , 317%. Increasing RoR to 300 mm decreased  $[\alpha_2] = [180^\circ]$  sensitivity by approximately 12%; all other configurations were decreased by approximately 75% of their 250-mm RoR sensitivities. Decreasing the acceptance angle to  $45^\circ$  decreased sensitivities to  $[\alpha_2, \alpha_3] = [120^\circ, 240^\circ]$ , 100%;  $[\alpha_2, \alpha_3] = [90^\circ, 180^\circ]$ , 105%; and  $[\alpha_2, \alpha_3, \alpha_4] = [90^\circ, 180^\circ, 270^\circ]$ , 210%. The 2-head  $[\alpha_2] = [180^\circ]$  system sensitivity was not affected. The configuration was the most important factor affecting the shape of the sensitivity profiles. For a 250-mm RoR and  $90^\circ$  acceptance angle,  $[\alpha_2] = [180^\circ]$  concentrated sensitivity in the FoV center,  $[\alpha_2, \alpha_3] = [120^\circ, 240^\circ]$  had a slightly increased peripheral sensitivity, and the profiles for both  $[\alpha_2, \alpha_3] = [90^\circ, 180^\circ]$  and  $[\alpha_2, \alpha_3, \alpha_4] = [90^\circ, 180^\circ, 270^\circ]$  were completely flat. **Conclusion:** Sensitivity profiles are affected strongly by imaging parameters; however, profiles can be shaped to concentrate on an annulus or distribute sensitivity uniformly over the FoV. Also, the 4-head system showed a markedly higher sensitivity than either of the 3-head systems.

**Key Words:** hybrid PET; gamma camera

**J Nucl Med 2001; 42:1116–1120**

---

**D**edicated PET with  $^{18}\text{F}$ -FDG has been used in oncology principally at different stages of diagnosis, staging, and therapeutic intervention (1). The high cost of dedicated

PET, as well as the success of FDG imaging, induced gamma camera manufacturers to adapt their relatively inexpensive dual-head gamma cameras to perform PET imaging (2). These cameras were designed originally for SPECT, but they can be used for PET with the addition of coincidence electronics. The principle of operation for hybrid PET systems is similar to dedicated PET: two opposing  $\gamma$ -rays are emitted from the site of positron-electron annihilation. If both  $\gamma$ -rays are detected simultaneously, the site of the positron-electron annihilation can be determined as being along a line of response (LoR) between the locations of the two detection events. From a tomographic perspective, the number of counts within a given LoR can be viewed as the projection of the activity distribution within the patient along this LoR.

However, one of the principal limitations that arose from hybrid PET design was a significantly inferior sensitivity (2,3). This constraint has limited these systems to applications with high uptake, such as myocardial imaging, or applications with potentially high contrast, such as oncology (4). The sensitivity of a hybrid PET system suffers from two penalties. The first arises from the use of large crystals. Although using large crystals reduces the cost, their use places higher demands on detection and positioning electronics. The photon detection load placed on the parallel operation of multiple small detectors in dedicated PET is assumed by one large detector in hybrid PET, leading to increased dead time. The second source of reduced sensitivity arises from the gap between detectors, which, as will be shown, reduces geometric sensitivity. Poor geometric sensitivity is most obvious in two-head hybrid PET designs. Typically, the heads are separated by  $180^\circ$ , covering only approximately half of the total angular range with the crystal. Because photons are emitted isotropically, using two heads fails to detect a good portion of the photon flux. One way to improve the angular coverage is by adding a third detector head so that coincident events occurring between any pair would be accepted (5). Recent limited testing by the National Electrical Manufacturers Association showed this increased sensitivity (6). Another method of reducing the gap between cameras is to use a curved crystal (7).

The multihead geometry of hybrid PET results in a non-uniform sampling of LoRs across the field of view (FoV). Camera rotation makes the sampling more uniform; how-

---

Received Nov. 27, 2000; revision accepted Mar. 5, 2001.

For correspondence or reprints contact: Robert Stodilka, PhD, Radiation Effects Group, Defense Research Establishment Ottawa, 3701 Carling Ave., Ottawa, Ontario, Canada, K1A 0Z4.

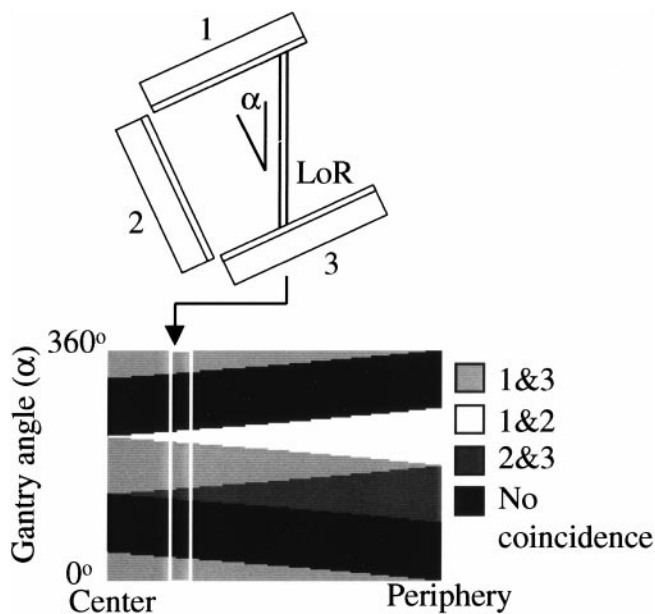


**FIGURE 1.** Sensitivity sinogram plots gantry angle  $\alpha$  vs. LoR radial position. Plot indicates which pairs of gamma cameras are intersected jointly by LoR. Sensitivity sinogram can be summed along columns (summed along  $\alpha$ ) to produce sensitivity profile, such as shown in Figures 3–6.

ever, sensitivity still varies across the FoV. For two-head detectors placed  $180^\circ$  apart, the sensitivity is greatest in the FoV center (8), whereas for a three-head camera, with detectors placed in an equilateral triangle, the sensitivity is peaked in the FoV periphery (5,9,10).

Nonuniform sensitivity profiles have important implications for estimation tasks (11,12) and may well affect lesion detectability. Because the performance, and ultimately the value, of hybrid PET is so often questioned, particularly because of limited sensitivity, it becomes important to understand how this characteristic is related to imaging parameters.

Sensitivity profiles in hybrid PET are dependent on several imaging parameters. During data acquisition, the sensitivity profile is determined by the number of heads, their angular separation about the axis of rotation, their radii of rotation and size, and the number of gantry stops. After acquisition, the sensitivity profile can be further affected during rebinning by restricting the maximum allowable angle of acceptance, that is, the angle between a coincident LoR and the camera face perpendicular.

Previous studies have described sensitivity profiles for continuously rotating dual-head detectors (13,14) and, more generally, circularly symmetric sensitivity profiles. Current industry products and future directions, however, lean toward using discrete gantry stops and possibly severely reducing the number of gantry stops (15). Reducing the number of gantry stops may introduce sensitivity-related artifacts during reconstruction (16). Part of this study will investigate the implications of reducing the number of gantry stops.

## MATERIALS AND METHODS

The geometric sensitivity of an LoR is proportional to the amount of time that it jointly intersects the FoV of any two gamma cameras, notwithstanding additional restrictions caused by reduced acceptance angles. Computer simulations were performed to calculate the sensitivity for each LoR. The sensitivity for a given LoR was calculated by rotating the gantry in discrete steps and counting the number of steps in which the LoR could be measured. LoRs were defined to be 1-dimensional lines spaced 1 mm apart. For a LoR to be measured at a particular gantry position, it must simultaneously intersect any 2 cameras and fall within the acceptance angle of both cameras. In 3- and 4-head systems, different combinations of gamma cameras may contribute to the same LoR as the gantry rotates. This information can be visualized by the geometric sensitivity sinogram, as shown in Figure 1.

Geometric sensitivity is determined by the number of heads, head size and configuration, radius of rotation (RoR), coincident head acceptance angle, and angle spacing between gantry stops. This study compared the performance of 2-, 3-, and 4-head systems, with each head being 500 mm across. Unless otherwise specified, calculations assumed that data were acquired by rotating each head through  $360^\circ$  in 128 gantry stops. Sensitivity profiles were compared directly by plots and areas under plots.

Various configurations were modeled for each system. The system configuration was identified by the angle(s)  $[\alpha_n]$ , which described the angular separation between head 1 and head  $n$ . For example, a 3-head detector, with the heads in an equilateral triangle configuration, was described by  $[\alpha_2, \alpha_3] = [120^\circ, 240^\circ]$ . The configurations of interest are illustrated in Figure 2.

The effects of RoR and finite acceptance angle were also examined. The acceptance angle is the maximum deviation from

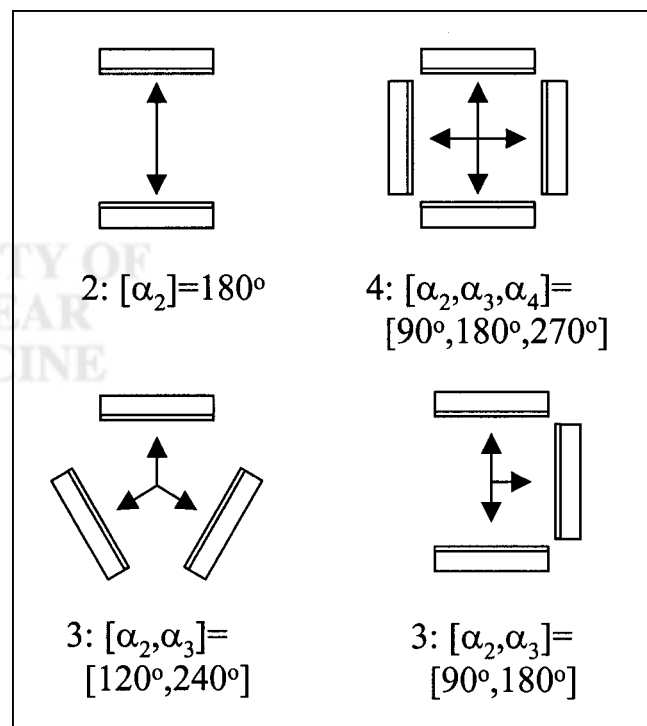


**FIGURE 2.** Four hybrid PET configurations were studied. Configuration is described by angle(s) defining angular separation between heads, as noted below each diagram.

the camera perpendicular that is permitted for an LoR to be counted. These two parameters were investigated separately by perturbing the system from the default parameters of 250-mm RoR and 90° acceptance angle. Further, only a subset of configurations was studied:  $[\alpha_2] = [180^\circ]$  for 2-head systems,  $[\alpha_2, \alpha_3] = [120^\circ, 240^\circ]$  and  $[90^\circ, 180^\circ]$  for 3-head systems, and  $[\alpha_2, \alpha_3, \alpha_4] = [90^\circ, 180^\circ, 270^\circ]$  for 4-head systems. Two RoRs were considered: 250 and 300 mm. Four acceptance angles were studied: 90°, 45°, 23°, and 11°. The acceptance angle was measured from the perpendicular of the camera face.

The results from these methods hold for the specific case of having the number of gantry stops equal to the number of rebinned projections. In general, however, this need not be the case, because multiple projections (or portions thereof) can be collected from a single gantry stop, limited by the acceptance angle. The effects of having fewer gantry stops than rebinned projection angles were examined for the 2-head  $[\alpha_2] = [180^\circ]$  configuration with a 250-mm RoR and 90° acceptance angle. This case was studied by reducing the number of gantry stops to 16 while still rotating each head through 360° and assuming 128 rebinned projections.

## RESULTS

Sensitivity profiles for each configuration, using 250-mm RoRs and 90° acceptance angles, are plotted in Figure 3. The plot shows the amount of time a LoR would be imaged for 360° rotation of the gantry in 128 steps. The sensitivity profile for the two-head configuration was shaped triangularly, and it concentrated sensitivity in the FoV center, whereas peripheral sensitivity was poor, dropping to zero at

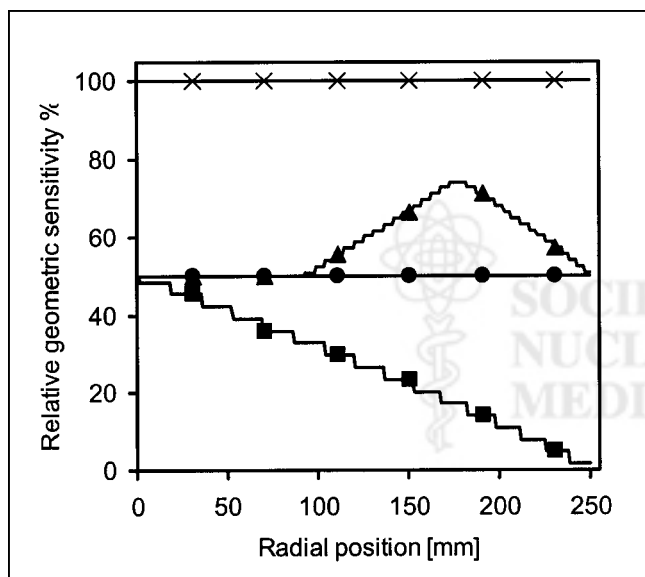


**FIGURE 3.** Sensitivity profiles for each configuration, assuming 250-mm RoR, 90° acceptance angle, and 128 gantry stops over 360° of gantry rotation. Profiles show percentage time that LoR, at given radial position, would image FoV. Two-head sensitivity profile (■) is peaked at FoV center, whereas 3-head  $[\alpha_2, \alpha_3] = [120^\circ, 240^\circ]$  profile (▲) is peaked at periphery. Both three-head  $[90^\circ, 180^\circ]$  (●) and 4-head (×) configurations have flat sensitivity profiles; however, 4-head profile shows twice the sensitivity of 3-head profile. Stepped appearance is caused by finite number of gantry stops.

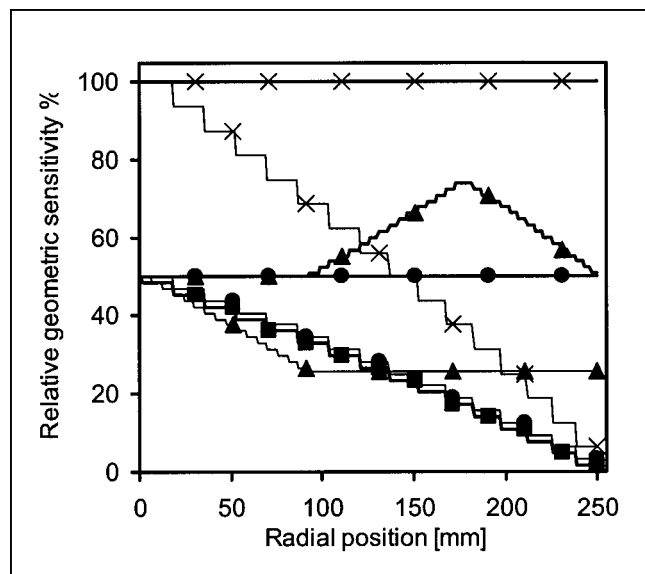


**FIGURE 4.** Each configuration with full 90° acceptance angle (thick lines) and reduced 45° acceptance angle (thin lines). Two-head profile (■) remains relatively unaffected. Profiles for 3-head  $[\alpha_2, \alpha_3] = [120^\circ, 240^\circ]$  (▲), 3-head  $[90^\circ, 180^\circ]$  (●), and 4-head configurations (×) show significant loss of sensitivity. This result is mainly caused by decreased coincidence between adjacent heads.

the FoV edge. Peripheral sensitivity was increased markedly by adding a third head, in either  $[\alpha_2, \alpha_3] = [120^\circ, 240^\circ]$  or  $[90^\circ, 180^\circ]$  configurations. Both 3-head configurations had identical sensitivities in the FoV center. The  $[90^\circ, 180^\circ]$  sensitivity profile was flat across the entire FoV, whereas the  $[120^\circ, 240^\circ]$  configuration offered increased sensitivity in the periphery. The 4-head profile was flat across the entire FoV, indicating that all LoRs were imaged during the entire acquisition.

The effect of decreasing acceptance angle is shown in Figure 4. In the figure, the 2-head profiles for acceptance angles of 90° and 45° are shown to be identical. Interestingly, this same profile is shared by a third configuration, namely, the 3-head  $[90^\circ, 180^\circ]$  case with a 45° acceptance angle, in which the smaller acceptance angle restricts coincidence to being between the 2 opposing heads. This same effect is evident in the 4-head case, in which the 45° acceptance angle prevents adjacent heads from accepting coincident photons, leaving only opposing heads accepting photon pairs. Thus, the 4-head sensitivity profile becomes exactly twice the 2-head profile. The 3-head  $[120^\circ, 240^\circ]$  profile is seen to drop significantly in sensitivity in the peripheral FoV. However, a small sensitivity advantage is noted over the 2-head profile (and, equivalently, the 3-head  $[90^\circ, 180^\circ]$  profile) in the peripheral FoV.

Two RoRs were simulated: 250 and 300 mm; these are compared for all configurations in Figure 5, assuming a 90° acceptance angle. In general, increasing the RoR decreased sensitivity across the entire FoV. This decrease was approximately uniform across the FoV. Thus, the characteristics of

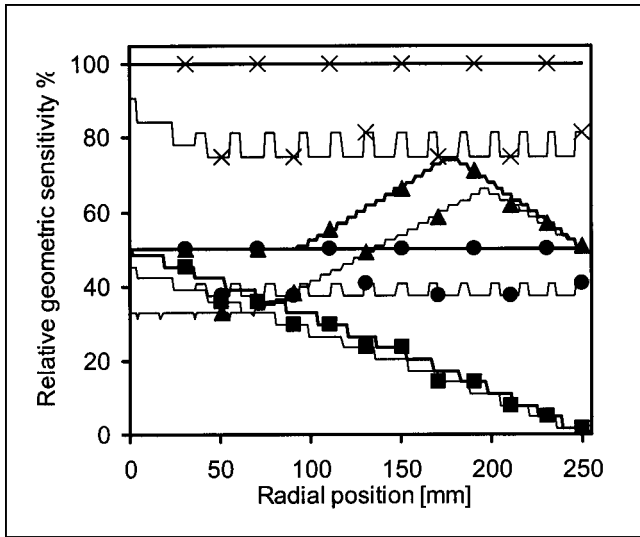


**FIGURE 5.** Increasing RoR decreased sensitivity. Sensitivity profiles from 250-mm (thick lines) and 300-mm (thin lines) RoRs are shown for each configuration. As with reducing acceptance angle, 2-head profile (■) remains least affected. However, profiles for 3-head [ $\alpha_2, \alpha_3$ ] = [120°, 240°] (▲), 3-head [90°, 180°] (●), and 4-head (×) configurations show loss of sensitivity. This loss is approximately uniform across FoV.

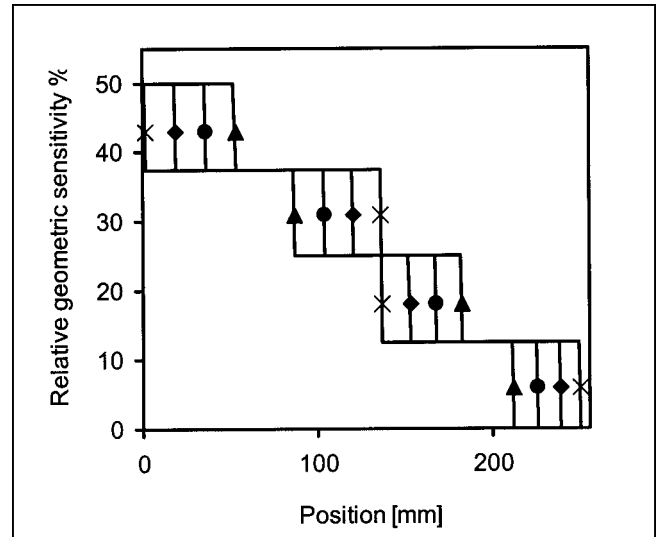


**FIGURE 6.** Effect of reducing number of gantry stops from 128 to 16 for 2-head configuration, assuming 250-mm RoR, 90° acceptance angle, and 128 rebinned projections over 360°. Sensitivity profile for these parameters is projection dependent. Profiles for first 4 rebinned projections are illustrated: projection at 0° (×), projection at 2.8° (◆), projection at 5.6° (●), and projection at 8.4° (▲).

the sensitivity profiles for all configurations were maintained as the RoR increased.

The effects of varying the RoR and the acceptance angle for each configuration are summarized quantitatively in Table 1. Sensitivities are presented relative to the two-head configuration with a 90° acceptance angle and 250-mm RoR. If the acceptance angle decreased, the 3-head [90°, 180°] configuration approached the sensitivity of the two-head configuration, whereas the 4-head configuration approached twice the 2-head sensitivity, as predicted from Figure 4.

These results assumed that the number of gantry stops was equal to the number of rebinned projections. Figure 6 shows the effects of reducing the number of gantry stops to 16 while maintaining 128 rebinned projections over 360°.

**TABLE 1**  
Geometric Sensitivities for Hybrid PET Systems

Configuration	RoR (mm)*				
	250 (90)	300 (90)	250 (45)	250 (23)	250 (11)
[ $\alpha_2$ ] = [180°]	100	87.7	100	76.0	44.5
[ $\alpha_2, \alpha_3$ ] = [120°, 240°]	183	140	100	0	0
[ $\alpha_2, \alpha_3$ ] = [90°, 180°]	159	124	105	76.0	44.5
[ $\alpha_2, \alpha_3, \alpha_4$ ] = [90°, 180°, 270°]	317	247	210	152	89

\*Acceptance angles (deg) are given in parentheses.

Geometric sensitivities were integrated between center of rotation and 200 mm radially as percentage relative to [ $\alpha_2$ ] = [180°] (250-mm RoR, 90° acceptance angle).

The figure shows that the sensitivity profile quantizes to fewer levels. Further, the sensitivity profile varies, depending on the relative position of the gantry stop and rebinned projection. This variation is seen as a shift in the locations of the steps but does not change their levels.

## DISCUSSION

Sensitivity profiles vary among hybrid PET systems. Two-head systems tend to concentrate sensitivity in the center of the FoV. Sensitivity is more uniformly distributed for 3- and 4-head systems. For the 3-head system, the [ $\alpha_2, \alpha_3$ ] = [90°, 180°] configuration features a flat sensitivity profile across the FoV, whereas the [120°, 240°] configuration increases peripheral sensitivity (at the expense of slightly decreased central sensitivity). The 4-head system has a fairly uniform sensitivity profile across the entire FoV.

The selection of an optimal sensitivity profile is an unresolved issue. Estimation–task studies with both SPECT (11) and hybrid PET (12) have indicated advantages in shaping sensitivity profiles to counteract attenuation, that is, sensitivity profiles that are maximum in the center of the FoV. This argument can be extended to possibly increasing lesion detectability by shaping profiles to maximize sensitivity in regions of interest, especially because sensitivity profiles could be made to vary with the projection angle. However, in practice, neither lesion locations nor body contours should be assumed a priori.

An important caveat beyond the scope of this study is resolution. This limitation becomes apparent when considering that photons with large incident angles are more likely to be mispositioned because of limitations in measuring the

depth of interaction. Glick and Stodilka (17) and Vandenberghe et al. (18) showed that reducing the acceptance angle could lead to improved resolution, albeit at the expense of sensitivity (Fig. 4; Table 1). Thus, although a feature of the 3-head [90°, 180°] system is a uniform sensitivity profile, it may suffer from degraded resolution, because coincidences between adjacent detectors would have at least 1 incident angle >45°. Vandenberghe et al. (18) showed that the average tomographic spatial resolution for the [0°, 180°] configuration is approximately 15% and 30% better than those recorded with [90°, 180°] and [120°, 240°], respectively.

Reducing the number of gantry stops has 2 potential consequences. First, discretizing gantry positions quantizes sensitivity profiles to discrete levels but does not affect the dynamic range. Reducing the number of gantry levels reduces the number of discrete levels in the sensitivity profile. Second, the assumption of circularly symmetric rotational weights (5,10,13,14) breaks down when the number of rebinned projection angles is less than the number of gantry stops. The effect is seen as a shift in the sensitivity profile (Fig. 6). The magnitude of the effect increases with fewer gantry stops, because sensitivity profiles quantize to fewer levels. Therefore, the importance of calculating projection-dependent sensitivity profiles increases as the number of gantry stops is reduced.

This study focused on aspects of comparing sensitivity profiles in a single axial plane. The results would be most applicable for systems with restricted axial acceptance, the restriction being realized either physically through slat collimators or in postprocessing during rebinning. Although sensitivity is axially variant, this variation is similar among all configurations because sensitivity peaks at the center of the FoV. Reader et al. (14) provided a 3-dimensional analysis, although that study was limited to the 2-head [ $\alpha_2$ ] = [180°] configuration. Future studies could focus on a comprehensive analysis of the 3-dimensional characteristics of sensitivity profiles.

## CONCLUSION

The sensitivity profile for hybrid PET is highly variable across the FoV. The overall profile shape is determined largely by the angular separation between the heads. The other defining factors, namely, RoR, photon acceptance angle, and number of gantry stops, are not as influential in determining the profile. The typical 2-head configuration, with the heads being separated by 180°, provides the least uniform profile, being peaked centrally and dropping linearly to near zero in the peripheral FoV. Sensitivity profiles

for 3- and 4-head systems were found to be more uniform and offered considerably more sensitivity than the 2-head system. However, 3-head systems require large photon acceptance angles to realize increased sensitivity.

## ACKNOWLEDGMENTS

The authors thank Drs. Howard Gifford, Michael King, Manoj Narayanan, Hendrick Pretorius, and Glenn Wells and Mr. Luc Bouwens for many useful discussions. This study was supported in part by grant CA-78573 from the National Cancer Institute.

## REFERENCES

- Rigo P, Paulus P, Kaschten BJ, et al. Oncological applications of positron emission tomography with fluorine-18 fluorodeoxyglucose. *Eur J Nucl Med.* 1996;23:1641-1674.
- Lewellen TK, Miyaoka RS, Swan WL. PET imaging using dual-headed gamma cameras: an update. *Nucl Med Commun.* 1999;20:5-12.
- Coleman RE. Camera-based PET: the best is yet to come. *J Nucl Med.* 1997;38:1796-1797.
- Jarritt PH, Acton PD. PET imaging using gamma camera systems: a review. *Nucl Med Commun.* 1996;17:758-766.
- Matthews CG. Triple-head coincidence imaging. In: *Conference Record of the 1999 IEEE Nuclear Science Symposium and Medical Imaging Conference.*
- Vandenberghe S, D'Asseler Y, Koole M, Van de Walle R, Lemahieu I, Dierckx RA. Physical evaluation of 511 keV coincidence imaging with a gamma camera. In: *Conference Record of the 1999 IEEE Nuclear Science Symposium and Medical Imaging Conference.*
- Adam LE, Karp JS, Daube-Witherspoon ME. Evaluation of performance of the CPET scanner using standardized measurement techniques. In: *Conference Record of the 2000 IEEE Nuclear Science Symposium and Medical Imaging Conference.*
- Clack R, Townsend D, Jeavons A. Increased sensitivity and field of view for a rotating positron camera. *Phys Med Biol.* 1984;29:1421-1431.
- Stodilka RZ, Glick SJ. Optimizing geometry for hybrid PET: dual-, triple-, and four-head cameras [abstract]. *J Nucl Med.* 2000;5(suppl):176P.
- D'Asseler Y, Vandenberghe S, Koole M, et al. Geometric sensitivity calculation of three-headed gamma camera-based coincidence detection. *Proc SPIE.* 2000;3977:58-67.
- Kijewski MF, Muller SP, Moore SC. Nonuniform collimator sensitivity: improved precision for quantitative SPECT. *J Nucl Med.* 1997;38:151-156.
- Stodilka Z, Glick SJ. Comparison of dual- and triple-head hybrid PET systems using estimation task performance. In: *Conference Record of the 2000 IEEE Nuclear Science Symposium and Medical Imaging Conference.*
- Swan WL, Vannoy SD, Harrison RL, Miyaoka RS, Lewellen TK. Randoms simulation for dual-head coincidence imaging of cylindrically symmetric source distributions. *IEEE Trans Nucl Sci.* 1999;46:1156-1164.
- Reader AJ, Erlandson K, Flower MA, Ott RJ. Fast accurate iterative reconstruction for low-statistics positron volume imaging. *Phys Med Biol.* 1998;43:835-846.
- DiFilippo FP, Gagnon D. *Partial Angle Tomography Scanning and Reconstruction.* US Patent 5923038, 1997.
- Kadmas DJ, Di Bella EV. Fully-3D binning and Fourier space rebinning of PET data acquired with rotating planar detectors [abstract]. *J Nucl Med.* 2000;5(suppl):196P.
- Glick SJ, Stodilka RZ. The effect of photon incidence angle on spatial resolution with thick crystal hybrid PET [abstract]. *J Nucl Med.* 2000;5(suppl):56P.
- Vandenberghe S, D'Asseler Y, Matthews CG, et al. Influence of detector thickness on resolution in three-headed gamma camera PET. In: *Conference Record of the 2000 IEEE Nuclear Science Symposium and Medical Imaging Conference.*